

COMPUTATIONAL ELECTROMAGNETIC MODELING AND EXPERIMENTAL VALIDATION OF FUEL TANK LIGHTNING CURRENTS FOR A TRANSPORT CATEGORY AIRCRAFT

D. Lalonde*, J. Kitaygorsky †, W. Tse*, S. Brault*, J. Kohler*, C. Weber †

*Bombardier, Canada, david.lalonde@aero.bombardier.com, †Electromagnetic Applications Inc., USA, jennifer@ema3d.com

Keywords: Aircraft, Lightning, Indirect Effects, Fuel Tank, Computational Electromagnetics

1 Abstract

A full scale aircraft lightning test campaign was conducted to support compliance with AWM 525.981 through validation of computational electromagnetic (CEM) models. The aircraft is injected with different lightning current attachment scenarios while measurements of currents, voltages and magnetic fields focused in the composite wing area. The high fidelity aircraft model has been resolved with EMA3D software. It includes accurate structural features, fasteners, wiring and systems tubing. The overall comparison between the full scale test results and the simulation results is very good both for the shape and the amplitude of the waveforms.

2 Introduction

Each lightning strike configuration on an aircraft produces a specific structural current distribution from the entry point to the exit point. This current distribution depends on structure electrical conductivity and most importantly that of fastened joints. Indirect effects of lightning are also observed by means of current and voltage induced on systems wiring and tubing.

Design features in the aircraft fuel tank shall prevent ignition due to high currents and voltages that can result in sparking. In addition, aircraft compliance with AWM 525.981(a)(3) [1] (and 14 CFR 25.981(a)(3) [2]) requires consideration of failure modes for both systems and structure design such that lightning direct effects testing is conducted on representative sub-assemblies that contain the failures. It is then essential to establish the aircraft lightning environment (threat levels) within the fuel tank structure to show it will not be of sufficient amplitude to cause ignition.

Definition of the threat levels can be supported by simulation and analysis, through a well-defined process of verification and validation that follows an increasing level of complexity, as shown in Figure 1. The use of simulation for determining Actual Transient Levels (ATL) is described in [3] while some applications are described in [4, 5, 6]. Generally, simulation tools provide more extensive means to rationalize threat level

predictions than by using development testing alone, but also more extensive means to evaluate specific design features.

This paper describes the full scale aircraft lightning testing campaign that was conducted to support the validation of computational electromagnetic (CEM) models.

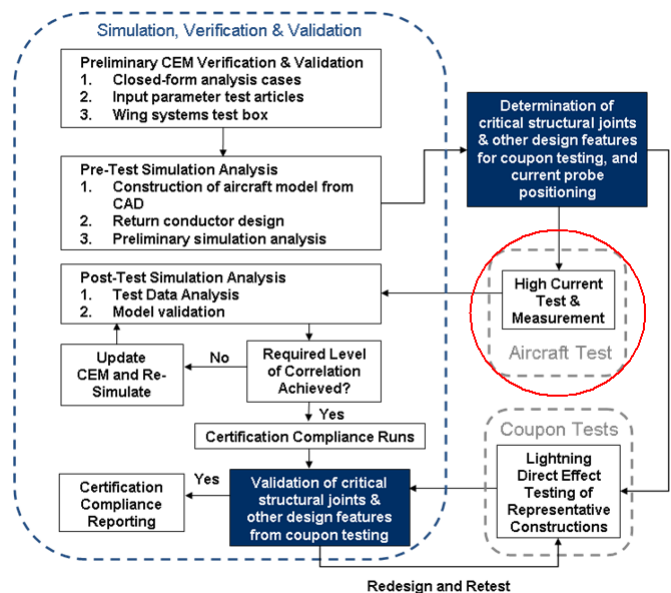


Figure 1. CEM Flowchart

3 Aircraft Test Campaign

Before testing, several lightning attachment scenarios were selected in an effort to obtain a sufficiently varied set of data and to represent some of the more probable in-service lightning attachments.

Preliminary simulation runs of all these attachments provided predictions of the expected threat levels in order to reduce the selection of attachments to a reasonable subset for aircraft testing. Consideration has been given for various threat level amplitudes, current paths in the fuel tank areas, but also for practicability of the lightning attachments during aircraft testing on ground. Table 1 shows the subset of lightning attachments selected for testing and validation.

Table 1. Lightning Current Attachments

| Attach location | Detach location |
|----------------------------------|-------------------------|
| Left hand side Wingtip | Right hand side Wingtip |
| Left hand side Main Landing Gear | Nose |
| Left hand side Engine | Aft Fuselage |

The aircraft was subjected to injection with low level scaled lightning current component A [7] and linearity verifications were performed to justify the subsequent extrapolation to full threat, similarly to what is described in [6]. The test peak amplitudes varied from about 3 kA to 15 kA.

As shown on Figure 2, and described in [8], a return conductor was built around the aircraft to mitigate the effect of the ground; effectively creating electromagnetic conditions that better represent an aircraft in-flight. It was connected at one end to the generator return and at the other end to the relevant current exit location on the aircraft. The effect of impedance of the aircraft and of the return conductor system (RCS) is of a slower injected waveform compared to a standard current component A. The time to peak (T1) of the waveform injected during test varied from about 14 to 24 μs depending on the attachment case instead of 6.4 μs specified in [7]. This slow injected waveform is a test limitation but it is replicated for validation as described in section 5.

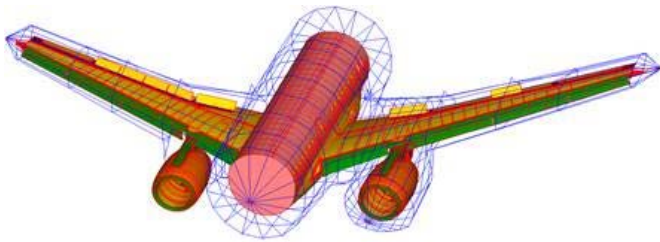


Figure 2. Return conductor system around the aircraft model

Measurements focused on the wing area and included bulk currents on harnesses and bonding straps, magnetic fields over the surface of structural components, structural voltages and pin open circuit voltages.

The magnetic field probes were designed and calibrated prior to the aircraft test campaign. The objective for aircraft model validation was to compare magnetic fields directly without any conversion to surface currents. This is a means to mitigate sources of discrepancies from such a conversion due to the complex geometric nature of the test article and the combined effect from many surrounding structural current orientations and amplitudes.

The test probes actually provide measurements of voltage across the probe winding according to Faraday’s Law of Induction, and numerical integration of this voltage is then multiplied by the relevant calibration factor. Equation (1) is the measured magnetic field, $H_{Measured}$, according to the probes calibration factors, F_{Cal} , measured voltage, $V(t)$, and time, t . Equation (2) is the equivalent summation for calculation.

$$H_{Measured} = F_{Cal} \int V(t)dt \quad (1)$$

$$H_{Measured} = F_{Cal} \sum_{i=1}^{\infty} v_i(t_i - t_{i-1}) \quad (2)$$

4 CEM Model

Simulations were performed with EMA3D, a finite-difference time-domain full wave solver, integrated with MHARNES, a transmission line solver. The 3D aircraft model, prepared with CADfix, included detailed features of the wings and the centre wing box but only parts of the fuselage to make its size more manageable. It also includes some details of systems routing and components. The model has a cell size of 25 mm and requires a total space size of about 5×10^8 cubic cells.

All probes are defined within the left wing fuel tank and the centre tank because the right wing is similar to the left wing. Therefore, the effect of the fuselage truncation on predictions of threat levels internal to the fuel tanks is expected to be minimal for all lightning attachments. Attachment to the nose and the tail of the aircraft connect to the truncated portions of the model but the current spreads to the full fuselage diameter before reaching the fuel tanks.

In order to control the impedance of structural joints, the model includes representative fastened joints in the form of joint surfaces and individual fastener representations. The modelling of those joints is shown in Figures 3 and 4, and was validated during the preliminary definition of input parameters, more specifically with the wing systems test box.

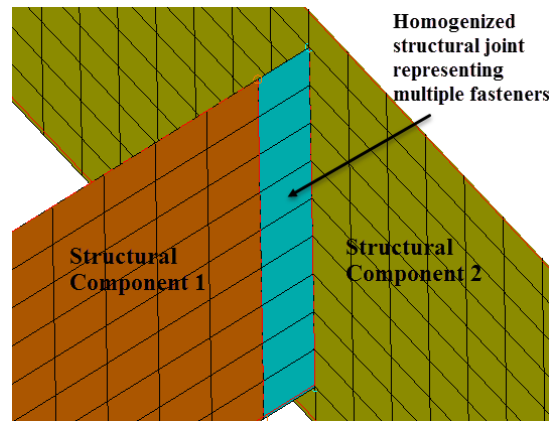


Figure 3: Joint surfaces representation

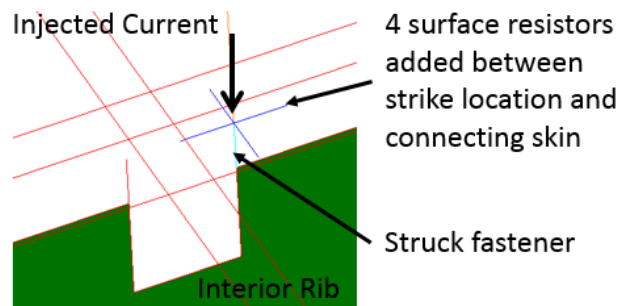


Figure 4: Individual fastener representation

Both representations are equivalent, but individual fasteners are preferred for local lightning attachment to those fasteners.

Electrical conductivities were also assigned to all structural components that are metallic or composite. The conductivity of composite materials included provisions for expanded copper foil when necessary, that is by considering the conductivity of the foil in parallel to composite. All prime material properties were obtained from input parameters test data (from previous steps shown in Figure 1) or technical specifications. When these sources were not readily available, material properties were determined by similarity or analysis.

The model was representative of the configuration of the aircraft during testing. The return conductor system has been represented and deviations compared to the pre-test model configuration were implemented, such as the position of the individual control surfaces, missing fasteners and access panels. Addition of structural gaps, when necessary, also permits to control the seam impedance and the predicted waveforms shape and amplitude by adding an inductive component.

The other structural joints are resistive but a structural gap then provides a means to control the time response of the CEM predictions. Gaps were used instead of joints only at the location of some access panels that shown missing fasteners and according to the geometry of the joints. No iterative dimensioning of these gaps was performed beyond this very specific application.

One of the most consequent model adjustments is of the fastener resistance depending on the nature of connecting materials. Previous steps in the project permitted to identify these input parameters specifically for this aircraft and for some main types of interfaces that include the following materials: composite, composite with expanded copper foil (ECF) and metal. Representing joints and individual fasteners are paramount for control of current distribution.

Another parameter that comes from preliminary steps in the project is the electrical conductivity for each type of material. It is known that composites exhibit anisotropic behaviour but the very complex nature of the aircraft model dictates the use of an equivalent isotropic representation instead. Comparison has been made between measured anisotropic values of some test samples, simulation models representing each directional layer of these panels (including the resin layers), and isotropic representations to provide equivalent bulk conductivities. The bulk conductivities were used for the full scale aircraft model.

Expanded copper foil also exhibits an anisotropic behaviour that depends on its diamond-shaped pattern as shown in Figure 5. This design feature is used on the aircraft to the best benefit from the privileged direction of electrical conductivity and based upon the specific design objectives. But again, the anisotropic behaviour is not directly represented in the model as it needs to be represented with a unique isotropic value.

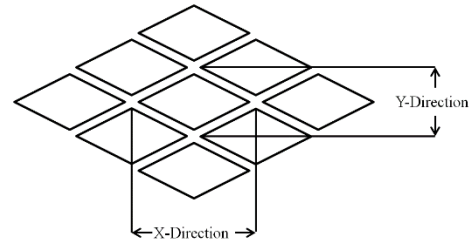


Figure 5. Expanded Copper Foil (ECF) Generic Pattern

The bulk conductivity representation for the expanded copper foil has been adjusted to be that of either the X or Y direction. The conductivity of composite with expanded copper foil (ECF) is then represented as a parallel combination of composite and ECF and is mainly driven by the metallic portion of the pair (ECF).

The aircraft model includes a set of probes to predict the same parameters as measured during aircraft testing, namely bulk current probes on harnesses and bonding straps, magnetic field probes over the surface of structural wing components, structural voltages and pin open circuit voltages.

5 Model Validation

Validation of the model is done through direct comparison of the measured and predicted values. These are the waveforms peaks for all types of measurements with the addition of action integral for currents. In the time domain, comparison of time to peak (T1) and time to half peak (T2) also provides valuable information during the process of model validation.

Figure 6 shows that injected test waveforms were numerically reproduced for the simulation runs but without the measured superimposed noise to mitigate numerical effects such as any unwanted oscillatory response. The injected waveforms are also scaled to full threat for the simulation model. That corresponds to a peak of 200 kA for current component A [7].

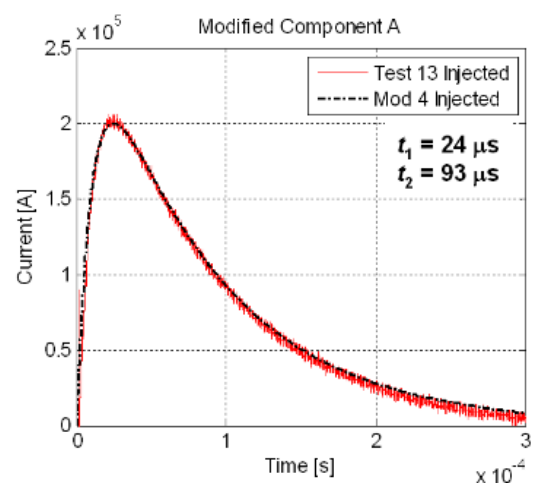


Figure 6. Injected current waveform scaled to full threat (Measured in red, Simulated in black)

But following model validation and as described in section 6, certification runs for the in-flight aircraft model use standard current component A with a faster time to peak.

The criteria used for model validation are described by the following breakdown:

1. A difference of 6 dB on peak in either direction was deemed acceptable.
2. No modification of CEM input parameters without a supporting rationale based upon test or engineering data, aircraft configuration, or engineering judgment.
3. Since some model modifications have more impact than others, a point is reached for the response to converge notwithstanding further and less significant modifications.

5.1 Currents

Figure 7 shows a typical comparison of measurements against CEM prediction for the current on a bonding strap.

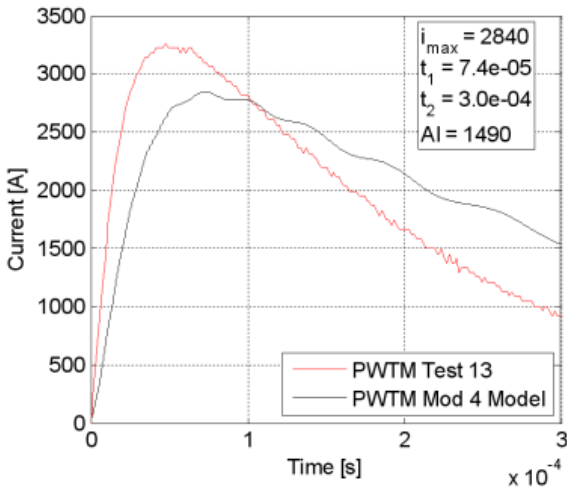


Figure 7. Current on bonding strap (Measured in red, Simulated in black)

The process of validation has been achieved while assessing the model response as a whole, e.g. considering the overall response of all probes in defining acceptable margins on CEM predictions in addition to evaluating individual probes.

The complexity of the model is such that it is reasonable to expect different levels of correlation depending on the probes location, whether it is on the main current path, its nature (the type of parameter it predicts) and whether its position pertains to structural features that are too localized to be effectively represented in the simulation model.

The overall correlation level between test measurements and CEM predictions for current peaks is shown in Figure 8.

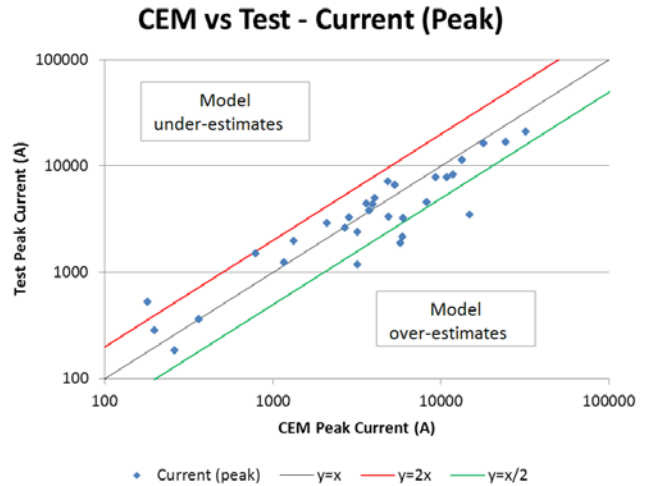


Figure 8. Scatter plot of currents (peak) comparison

It is observed that most of the predicted currents are within a margin of 6 dB from the test results. It has been observed that excursions outside of this margin were mainly coming from bundle currents on harnesses, or bonding jumpers in areas that are strongly influenced by complex joints like rotating joints and our relevant model assumptions.

Means to compare CEM predictions against test data is presented in [9, 10] through the “FSV” method and has been briefly investigated, but direct application to aircraft lightning problems was found to be “impractical” due to their relatively low frequency content. However, the core of the FSV method can be described as the comparison of amplitude and shape (feature) of a waveform. Due to the predictable nature of the lightning waveforms on the aircraft, the use of peak and action integrals is considered sufficient for comparison of the current waveforms amplitude and feature.

5.2 Voltages

The CEM voltage waveforms are showing more oscillations than test results such that numerical filtering is applied on CEM predictions to get the underlying waveform for comparison. Filtering is done using a simple moving average algorithm.

Equation (3), from [11], is the frequency response of a moving average filter, $H[f]$, according to the percentage of the CEM probes sampling frequency, f , and the number of points used for the moving average filter, M .

$$H[f] = \frac{\sin(\pi f M)}{M \sin(\pi f)} \quad (3)$$

As an example, the response for a CEM probe resolution of 1×10^{-8} s and 5 points moving average is shown on Figure 9.

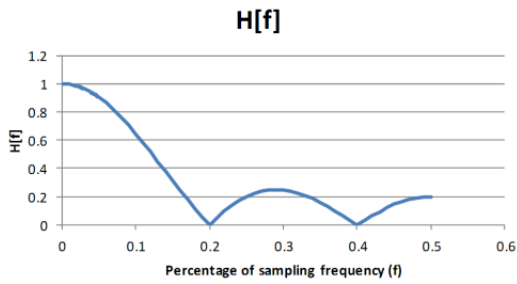


Figure 9. Frequency response of moving average filter

Comparison for voltages is achieved and the resulting scatter plot is shown in Figure 10.

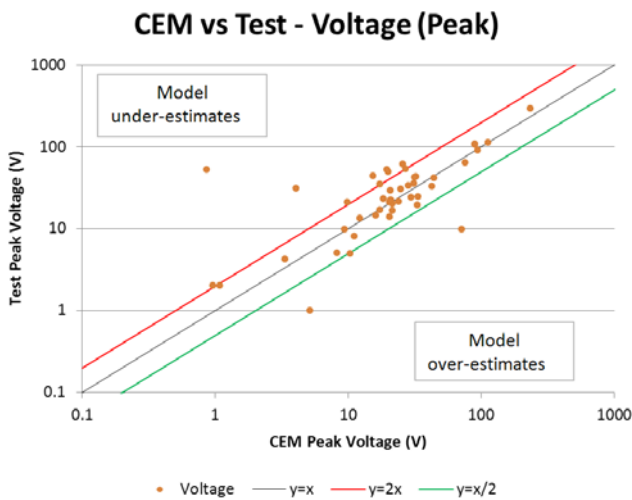


Figure 10. Scatter plot of voltages (peak) comparison

Most voltage predictions are crowded in Figure 10 due to their similar nature, e.g. mostly structural differential voltages, and most are within a 6 dB margin from the test results. It has been observed that excursions outside of this margin were mainly open circuit voltages on systems wiring.

Table 2 shows the time characteristics of standard voltage waveforms 2 and 4 [12].

Table 2. Voltage waveforms time characteristics [12]

| Waveform | Time to peak (T1) | Time to half peak (T2) |
|----------|-------------------|------------------------|
| 2 | 100 ns | 6.4 μs |
| 4 | 6.4 μs | 69 μs |

As described in [3], open circuit voltages on system routing going over structural openings would exhibit some waveform 2 content when the surrounding structure is metallic. It has been shown that resolution of such fast voltages is possible with this CEM model. It requires analysis over different options of the number of points for the average filter, but also the selection of a sufficiently fine solving resolution (CEM probes time step).

Some instances of composite waveforms that include some waveform 2 and waveform 4 content were observed for systems routing going over the wing tank access panels. For example, Figure 11 shows the early time response of these waveforms, for one CEM probe, by subsequent use of an increasing number of points for the moving average filter. Starting from raw CEM data, the response is filtered until the waveform content can be observed and described.

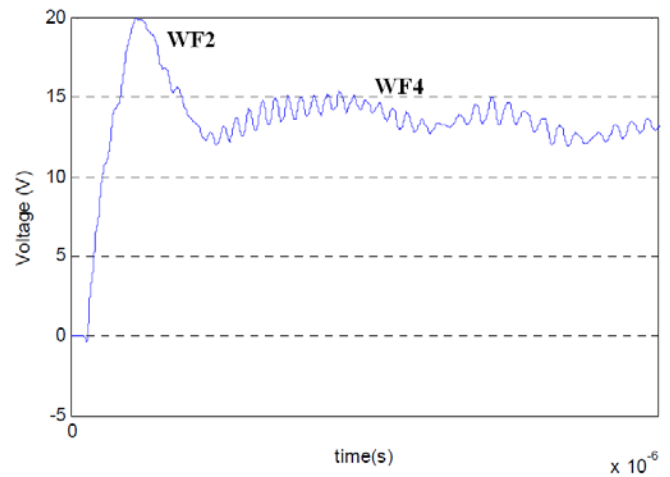


Figure 11. Resolution of WF2 and WF4 voltage waveforms

While the number of points is related to the cut-off frequency of the filter, which depends on the CEM probes resolution and needs to be sufficiently high to capture fast waveforms, the observation here is more about the means to use CEM for studying and describing the content of complex waveforms.

Considering all attachment cases and all types of probes, the observed level of correlation is such that over 80% of the CEM predictions fall within 6 dB of the measured data. Cases that fall outside of this 6 dB margin were investigated on a case-by-case basis in an effort to identify the most probable causes, including potential test uncertainties.

5.3 Harnesses (Wiring)

It has been observed that most (about 80%) of all predictions that fall outside of the 6 dB margin are harness currents and voltages. Some discrepancies are coming from the definition of the simulation probes in predicting the bundle current for particular branching configurations, especially in the vicinity of connectors. For other cases, it comes from discrepancies in bundle representation, transfer resistance assumptions or the bonding values of harness terminations. Transfer resistance for harnesses was initially represented following the process described here:

1. From the bundle diameter in CATIA, the number of conductors is estimated assuming only 1 conductor size and only twisted shielded pairs (commonality).
2. It is assumed that each harness has the same type of overbraid.

3. The transfer resistance of each bundle is estimated by calculating the parallel resistance that includes all twisted pairs and the overbraid.
4. Harnesses are all terminated with the same resistance to represent connector terminations.

The level of correlation achieved with these initial assumptions is considered excellent for predicting internal current distribution and voltages. But for lightning indirect effects on systems routing, more accurate development of the harnesses content has also been achieved subsequently for a subset of harnesses in the wing area such that each individual conductor is detailed with a higher degree of fidelity from each termination to the next.

Figure 12 is an example that shows predictions for one bundle current prediction that fell outside of the 6 dB margin during initial model validation. For this case, definition of the probe has been more accurately aligned with the test procedure for the bundle current around a specific branch of the harness and for the same exact routing and harness content.

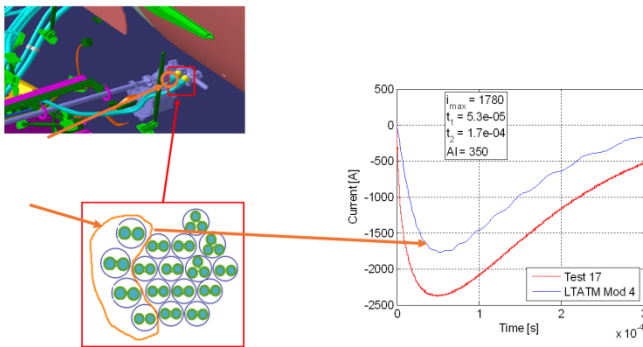


Figure 10. Bundle current prediction for accurate harness (Measured in red, Simulated in blue)

6 Certification Compliance Runs

Validation of the test aircraft model is only a preliminary step for the final certification runs in validating the model features and assumptions. For the certification runs, the equivalent in-flight aircraft model is used. The later includes all features of the test aircraft model except for the return conductor system that is shown on Figure 2.

The subset of 3 lightning attachments used for validation is extended substantially to more than 60 attachments for the certification runs in an effort to predict the worst possible threat level for each CEM probe. While the validation used slower injected waveforms, certification runs used standard current components depending on aircraft lighting zoning.

It is the level of correlation observed between the test results and the CEM predictions during validation that is used to define the margins to apply over the worst case predictions for each CEM probe. Specific margins are then applied on

CEM predictions of peak amplitudes but also on action integrals.

This approach yields a sufficient level of confidence and conservatism for definition of the threat levels for the test coupons. Combination of the extended lightning attachments and the observed validation margins provide threat levels that are sometimes noticeably higher than what has been observed from aircraft testing alone.

7 Conclusions

Compliance to AWM 525.981(a)(3) for fuel tank ignition prevention is being supported by means of Computational Electromagnetics. The full aircraft testing campaign has been conducted to support model validation through predictions of internal currents, voltages and magnetic fields. The overall comparison between the full scale aircraft test results and simulation is very good both for the shape and the amplitude of the waveforms. The very high level of details implemented in the simulation models, including but not limited to that of fastened joints, favoured the observation and validation of some behaviour of hybrid construction wing structures such as combined voltage waveform content. A detailed model also requires the definition of many input parameters. Those should be defined by means of specific testing and modelling, existing engineering data, or the impact of variables should be assessed by sensitivity analysis. It has also been observed that simple assumptions for the harnesses bundle content can provide a first range of values for induced lightning indirect effects but accuracy was increased with a more detailed description.

8 Acknowledgements

The content in this paper is a summary of the work done through a sizable collaborative effort. As such, Bombardier acknowledges the contributions of EMA Inc. for providing committed support during all simulation and test aspects of the project; NTS Lightning Technologies for its expertise and dedication in conducting the full aircraft lightning test; and all those who supported any or all aspects of this activity from a technical and/or logistic point of view.

9 References

- [1] AWM 525.981: 'Part V – Airworthiness Manual Chapter 525 – Transport Category Aeroplanes – Fuel Tank Explosion Prevention', TCCA, 2014-1
- [2] 14 CFR 25.981: 'Code of Federal Regulations – Title 14 Aeronautics and Space – Part 25 Airworthiness Standards: Transport Category Airplanes – Fuel Tank Ignition Prevention', FAA, May 21 2015
- [3] SAE ARP5415 Rev.A: 'User's Manual for Certification of Aircraft Electrical/Electronic Systems for the Indirect Effects of Lightning', 2002

- [4] Wahlgren, Bo. I., and Rosen, Jonas W., 'Finite Difference Analysis of External and Internal Lightning Response of the JAS39 CFC Wing'. International Aerospace and Ground Conference on Lightning and Static Electricity, Oklahoma City, USA, April 1988, pp. 396–400
- [5] Satake, K., Yamamoto, S., Yamakoshi, H., AOI, T., Iyomasa, A., and Murakami, K.: 'Development of Electromagnetic Simulation Supporting Lightning Protection Design of Mitsubishi Regional Jet', Mitsubishi Heavy Industries Technical Review Vol.49 No.4, 2012, pp.79–84
- [6] Atkins, A., Hardwick, J., Morgan, D., Terzino, N., Atkins, D., Flourens, F., and Simpson, H.: '106dB Current Linearity Study of the TANGO CFC Wingbox', Oxford, 2011
- [7] SAE ARP5412 Rev.A: 'Aircraft Lightning Environment and Related Test Waveforms', 2005
- [8] SAE ARP5416: 'Aircraft Lightning Test Methods', 2005
- [9] Duffy, A.P., Sasse, H.G., Archambault, B., and Drozd, A.: "Overview and Update on IEEE Std 1597.1 'Standard for Validation of Computational Electromagnetics Computer Modeling and Simulation'", Proceedings of the 59th International Wire & Cable Symposium, 2010, pp.69–76
- [10] IEEE 1597.1: 'IEEE Standard for Validation of Computational Electromagnetics Computer Modeling and Simulations', 2008
- [11] Smith, S. W.: 'The Scientist and Engineer's Guide to Digital Signal Processing' (California Technical Publishing, 1997, 2nd edn. 1999)
- [12] RTCA DO-160 Rev.F: 'Environmental Conditions and Test Procedures for Airborne Equipment', 2007